CVD Growth of 3C-SiC on 4H/6H Mesas

Dr. Philip G. Neudeck*
NASA Glenn Research Center at Lewis Field, 21000 Brookpark Road, M.S. 77-1
Cleveland, OH 44135, USA
Phone: (216) 433-8902, FAX (216) 433-8643, E-mail: Neudeck@nasa.gov

Andrew J. Trunek and David J. Spry
OAI, NASA Glenn Research Center, 21000 Brookpark Road, M.S. 77-1
Cleveland, OH 44135, USA

J. Anthony Powell
Sest, Inc., NASA Glenn Research Center, 21000 Brookpark Road, M.S. 77-1
Cleveland, OH 44135, USA

Hui Du and Prof. Marek Skowronski
Dept. of Material Science and Engineering, Carnegie Mellon University
Pittsburgh, PA 15213, USA

Dr. XianRong Huang and Prof. Michael Dudley
Dept. of Materials Science and Engineering, SUNY at Stony Brook
Stony Brook, NY 11794 USA

Abstract

This article describes growth and characterization of the highest quality reproducible 3C-SiC heteroepitaxial films ever reported. By properly nucleating 3C-SiC growth on top of perfectly

on-axis (0001) 4H-SiC mesa surfaces completely free of atomic scale steps and extended defects, growth of 3C-SiC mesa heterofilms completely free of extended crystal defects can be achieved. In contrast, nucleation and growth of 3C-SiC mesa heterofilms on top of 4H-SiC mesas with atomic-scale steps always results in numerous observable dislocations threading through the 3C-SiC epilayer. High-resolution X-ray diffraction and transmission electron microscopy measurements indicate non-trivial in-plane lattice mismatch between the 3C and 4H layers. This mismatch is somewhat relieved in the step-free mesa case via misfit dislocations confined to the 3C/4H interfacial region without dislocations threading into the overlying 3C-SiC layer. These results indicate that the presence or absence of steps at the 3C/4H heteroepitaxial interface critically impacts the quality, defect structure, and relaxation mechanisms of single-crystal heteroepitaxial 3C-SiC films.

Table of Contents Text

By properly nucleating 3C-SiC on top of a patterned array of (0001) 4H-SiC mesas with surfaces completely free of atomic scale steps, growth of 3C-SiC mesa heterofilms free of extended crystal defects can be achieved. Detailed characterization, including AFM, TEM, and X-ray, indicates that the presence or absence of steps at the 3C/4H interface critically impacts the quality, defect structure, and relaxation mechanisms of single-crystal heteroepitaxial films.

Keywords: 3C-SiC, heteroepitaxy, dislocations, mesa, surface steps

1. Introduction and Background

The chemical vapor deposition (CVD) technique is widely accepted as offering the most promise for well-controlled homoepilayer growth required for mass-production of most SiC electronic devices.[1,2] The variations of SiC CVD epitaxial growth, which are described in detail elsewhere in this special issue, rely on heating a 4H or 6H-SiC substrate to growth temperatures in excess of 1300 °C in the presence of flowing growth precursors containing silicon (often SiH_4) and carbon (often C_3H_8) containing gas species in a carrier gas (often H_2) at pressures at or below atmospheric pressure. However, the fact that SiC exhibits polytypism (i.e., comes in many different crystal structures with different electronic properties) imposes additional (compared to other semiconductor materials) considerations (described below and elsewhere in this special issue) in order to obtain CVD growth of sufficient quality crystal for electronic devices. As better described in previous publications,[1,3,4] the crystal structure of each polytype is described by a repeated stacking sequence of tetrahedrally bonded Si-C bilayers. The atoms in any bilayer can take on one of three positions (labeled as "A", "B", or "C") relative to other bilayers in the lattice. The cross-sectional structure and associated bilayer stacking sequences of the most commonly produced polytypes are shown in Fig. 1. 3C-SiC is the only SiC polytype with a cubic crystal structure, and thus is the only SiC polytype with four geometrically equivalent <111> stacking directions. There are two rotational variants of 3C-SiC, denoted as 3C(I) and 3C(II), that are related to each other by a 180° rotation about a stacking direction axis. The other SiC polytypes have only one stacking direction, the <0001> crystallographic c-axis. The close-packed planes (i.e., {111} for 3C-SiC and (0001) for the other SiC polytypes) normal to the stacking directions have the lowest defect propagation energies, and are thus most favorable for dislocation defect propagation.[3,5]

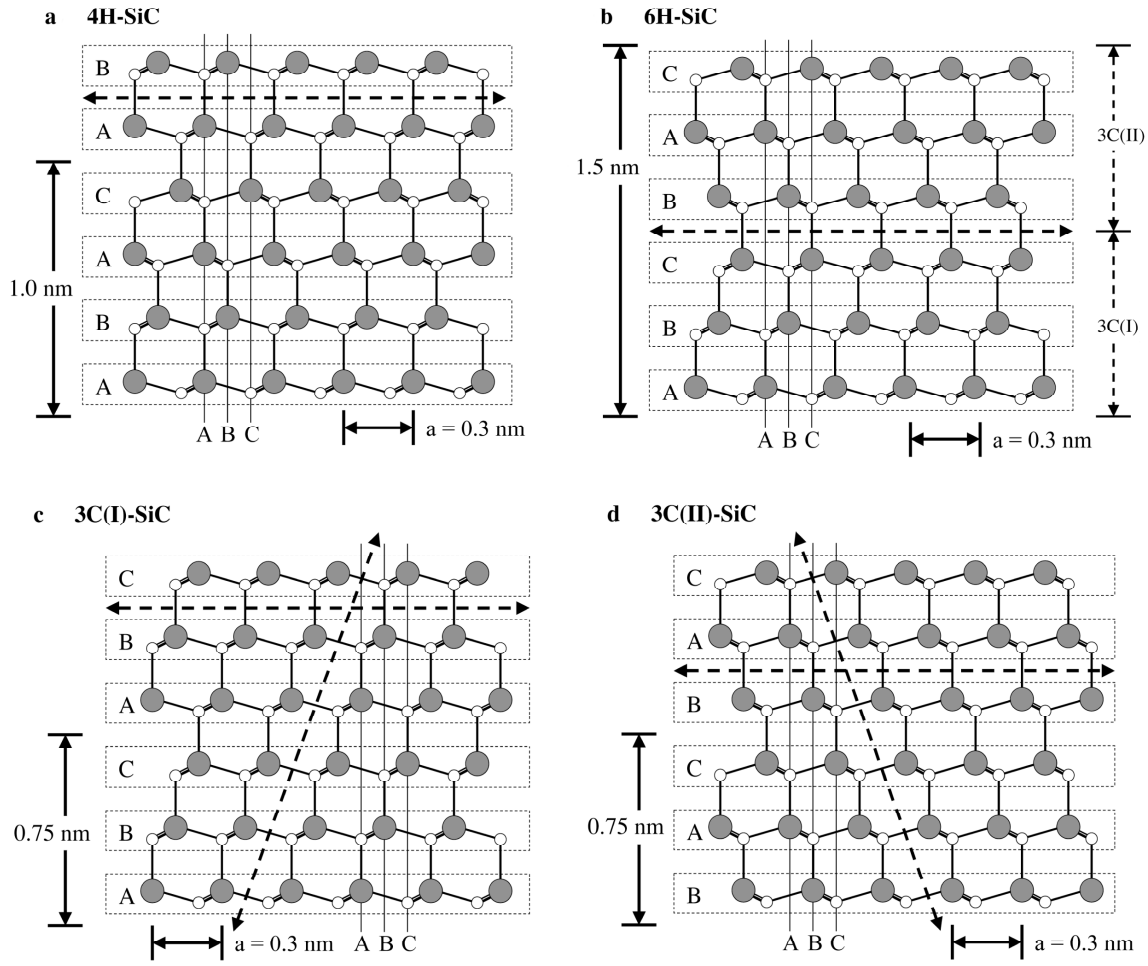

Fig. 1. Crystal structure of major SiC polytypes projected onto $(11\bar{2}0)$ or (110) planes.[17] The bilayer stacking sequence, c-axis stacking repeat height, in-plane lattice parameter (a = 0.3 nm), and corresponding lateral positions of silicon (dark) atoms are illustrated. The (0001) basal plane for 4H-SiC and 6H-SiC and two of the four equivalent (111) planes for 3C-SiC are illustrated by the dashed lines.

Presently, all commercialized SiC devices are implemented in homoepitaxial films of the 4H- and 6H-SiC polytypes grown on commercial SiC wafers with surfaces polished 3° to 8° off the (0001) basal plane.[1,2,4] This off-axis polish provides a high density of atomic surface steps, such as those depicted in the simplified schematic growth surface representation of Fig. 2. The high step density and small terrace width ensures migration of mobile surface-adsorbed growth adatoms to step edges where they incorporate into the crystal, as depicted on terrace (a) of Fig. 2.

This stepflow growth process used to grow 6H-SiC and 4H-SiC homoepilayers is often referred to as "step controlled epitaxy."[4,6-8] Homoepitaxy of 4H-SiC or 6H-SiC is kinetically controlled growth, in that it relies on lateral bilayer expansion (i.e., lateral stepflow) from existing substrate step edges for growth and structural stacking (i.e., polytype) replication.

When CVD reactor growth and/or SiC surface conditions deviate from nominal stepflow, growth adatoms can be incorporated into the crystal by forming islands in the middle of terraces, as depicted for terrace b of Fig. 2, instead of migrating to existing step edges. When this two-dimensional (2D) terrace nucleation occurs during CVD growth of SiC below 1700 °C, it is well documented that the terrace nucleated islands assume the 3C-SiC stacking structure.[4,6,7,9] Terrace nucleation can be promoted by conditions that reduce the probability that reactant adatoms successfully diffuse to step edges. Such conditions include higher supersaturation, lower growth temperature, the presence of surface defects and/or contamination, and/or longer terrace widths induced by "on-axis" (0001) wafer surface orientation.[4,6-8] The fact that terrace nucleation consistently produces the 3C polytype in conventional SiC CVD epitaxy processes

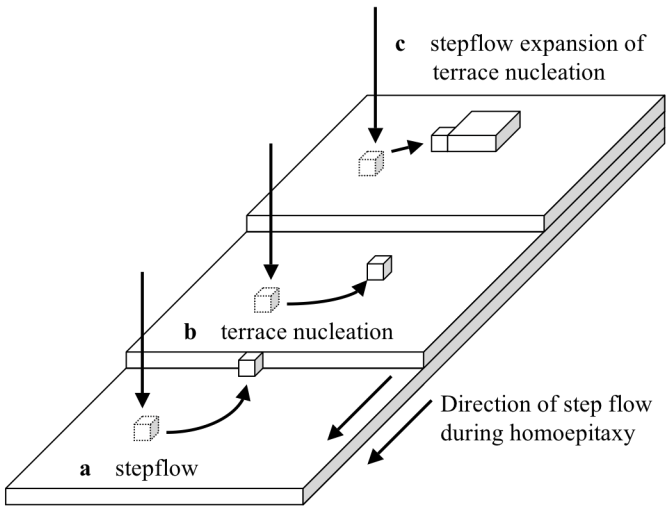

Fig. 2. Simplified schematic illustration of steps and adatoms on SiC epitaxial growth surface.[17]

indicates that the cubic bilayer stacking sequence is thermodynamically preferred for standard SiC epitaxial growth conditions. Such nucleation and growth is usually undesired, as it produces electrically harmful 3C-SiC poltype inclusions in otherwise uniform 4H-SiC or 6H-SiC device homoepilayers.

In CVD growth conditions where terrace nucleation dominates, a heteroepilayer of (111) oriented 3C-SiC can be grown on top of (0001) 4H- or 6H-SiC wafers. However, for reasons discussed later in this paper and elsewhere, these 3C layers have proven highly defective, generally containing dislocation densities more than 100-fold larger than high-quality 4H-SiC and 6H-SiC wafers and epilayers.[6,9-11] Similarly, 3C-SiC heteroepilayers grown on large-area silicon substrates (including improved 3C-SiC growth on "undulant silicon" discussed elsewhere in this special issue) to date also contain much higher dislocation densities than those routinely obtained in commercial 4H-SiC and 6H-SiC wafers and homoepilayers.[12] Lastly, previous efforts to grow bulk 3C-SiC crystals compatible with semiconductor electronics mass-production have also failed to yield acceptable crystal quality.[13]

Therefore, despite decades of 3C-SiC materials development effort, the theoretical potential of 3C-SiC electronic devices has gone largely unrealized on even a prototype experimental basis due to the lack of high-quality 3C-SiC crystal compatible with device fabrication. In particular, speculated device benefits with respect to MOSFET's (superior inversion channel mobility and reliability), bipolar transistors (superior reliability with lower on-state voltage), and heteropolytype junction transistor devices remain to be experimentally explored.[14-17]

Within the last few years, NASA Glenn Research Center has been pioneering on-axis CVD growth of SiC carried out on arrays of mesas patterned into commercial on-axis 4H- and 6H-SiC wafers.[17-21] These experiments have led to the first reported 3C-SiC films completely free of

dislocation defects over areas sufficient to support fabrication of dislocation-free 3C-SiC prototype electrical devices. This advancement, which we have named "step-free surface heteroepitaxy", is largely based upon properly controlling the SiC growth surface step structure to a degree not possible with off-axis wafer polish. In particular, controlled nucleation and growth of 3C-SiC on top of 4H-SiC or 6H-SiC mesas completely free of atomic-scale steps enables remarkable 3C-SiC film quality to be achieved. This article reviews present understanding of growth and defect-formation mechanisms revealed by this unique mesa growth approach to heteroepitaxy.

2. Results and Discussion

2.1 General 3C-SiC Mesa Heterofilm Film Growth Properties

The 3C-SiC mesa heterofilm growth process employed is respectively described and schematically illustrated later in the Experimental section. Noting that we have obtained similar results on 6H-SiC and 4H-SiC substrates, for clarity the remainder of this paper will only refer to the use of 4H-SiC substrates. The growth of the 3C-SiC layer usually takes place through terrace nucleation of new SiC bilayers on the mesa surface. In the absence of kinetic step-flow polytype control, thermodynamics dictates that the new terrace-nucleated SiC bilayers acquire cubic stacking. More specifically, we have shown that each new terrace-nucleated bilayer continues the local cubic stacking of the immediately underlying two bilayers.[17,18] Thus if the underlying two bilayers are stacked "AB", the new terrace nucleated bilayer will assume the "C" position to continue the "ABC" stacking of 3C(I) (Fig. 1). This enables a thick film of perfect 3C-SiC stacking (i.e., no hexagonal stacking) to be grown via further terrace nucleation. We have also shown that this thermodynamic stacking "selection rule" for new terrace-nucleated bilayers (in

CVD growth below 1700 °C) applies even when the two immediately underlying layers are the top two bilayers of a 4H-SiC or 6H-SiC crystal.[21] Therefore, the establishment of a step-free 4H- or 6H-SiC mesa surface, wherein the absence of steps guarantees that the top-most bilayers have the same stacking across the whole top surface of the mesa, effectively prevents opposite 3C rotational variants from terrace nucleating on that mesa surface. Furthermore, the step-free 4H-SiC surface enables unimpeded lateral stepflow enlargement of nucleated 3C-SiC bilayer islands to proceed free of collisions with laterally growing 4H-SiC crystal steps.

When the 4H-SiC mesa surface is not free of atomic scale steps, such as on a mesa threaded by an axial screw dislocation, the 3C-SiC film is observed to be highly defective. The collision of laterally expanding 3C-SiC islands and 4H-SiC growth steps is unavoidable in this

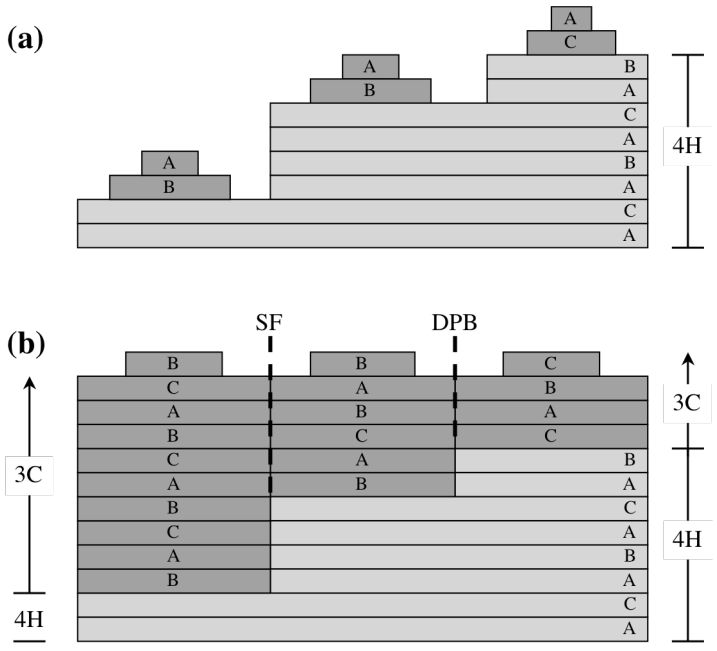

Fig. 3. Simplified cross-sectional depiction of mechanism for stacking fault (SF) and double-positioning boundary (DPB) defects can form on stepped 4H-SiC surface via island nucleation and stepflow expansion of bilayer steps. In contrast to previous models that propose random stacking due to terrace nucleation, stacking acquired during terrace nucleation in this model is thermodynamically well-controlled to continue the local cubic stacking sequence started by the immediately underlying two bilayers.

situation, resulting in defective merging of at least some bilayers with dissimilar stacking positions that result in dislocation defects. Terraces separated by step risers of 2 bilayers (0.5 nm) or 4 bilayers (1.0 nm) in height have been repeatedly observed on as-grown or as-stepflow-etched 4H-SiC surfaces, including the growth surrounding axial screw dislocations.[8,17,22] Fig. 3 simplistically illustrates examples of how such 4H-SiC step structure can produce double-positioning boundary (DPB) and stacking fault (SF) defects when growth via terrace nucleation (following the thermodynamic continuation of cubic stacking "selection rule") occurs on separate terraces of such a 4H-SiC growth surface.

Additional important 3C heterofilm extended defect formation mechanisms are discussed below in Section 2.2. It is important to note that the terrace nucleation probability (i.e. growth process conditions) can be adjusted such that terrace nucleation (i.e., 3C-SiC layer growth) occurs only on some fraction of mesas on a given sample. Such processes produced "mixed polytype" samples, wherein some fraction of mesas that do not experience terrace nucleation remain as homogenous 4H-SiC, other mesas experience only partial coverage of 3C-SiC, and other mesas are completely overgrown by 3C-SiC.[23] While not desirable for devices, such samples did enable useful direct side-by-side comparisons between 3C-SiC (hetero) film and 4H-SiC (homo) film properties, some of which are discussed in Section 2.2 below.

For step-free 4H/6H mesas, the stacking fault (SF) content of some 3C-SiC mesa films varied significantly as a function of 3C growth initiation process. 3C-SiC mesa heterofilms which were nucleated more slowly using gradual temperature ramp decreases exhibited higher SF-free yields than films nucleated with rapid temperature ramp decreases.[17,20] We proposed a growth model in which the low initial nucleation rate enables 3C-SiC heteroepitaxial growth to initiate and stepflow expand outward from a single 3C-SiC island, thereby eliminating SF-

defects associated with coalescence of multiple 3C-SiC islands expanding laterally on a step-free 4H-SiC mesa. We have theorized that the driving force for the defective 3C island coalescence leading to SF formation is in-plane lattice mismatch between the 3C-SiC film and the step-free 4H-SiC mesa. The coalescence of laterally expanding islands, albeit not necessarily on step-free substrate surfaces, is documented in other heterocrystal systems to form stacking faults.[24] Experimental measurements documenting non-trivial in-plane lattice mismatch and relaxation via misfit are reviewed later in Section 2.2.4.

2.2. Detailed Characterization of 3C-SiC Mesa Heterofilm Properties

The crystallographic structural properties of 3C-SiC heterofilms grown on stepped and un-stepped 4H- and 6H-SiC mesas have been extensively characterized by a variety of techniques. This section summarizes characterization results obtained to date and their relevance towards fuller understanding of growth and defect formation mechanisms of 3C-SiC heteroepitaxy. While these results have been largely consistent with the growth model described above, further experiments are required for more complete understanding of all aspects of the 3C-SiC heterofilm growth.

2.2.1. Confirmation of 3C-SiC Polytype

The independent methods of Synchrotron White Beam X-ray Topography (SWBXT), High Resolution X-ray Diffractometry (HRXRD), High Resolution Cross-sectional Transmission Electron Microscopy (HRXTEM), and thermal oxidation have been used to unambiguously confirm the 3C-SiC polytype of the mesa heterofilms.[21,25,26] These methods have demonstrated complete agreement on all samples studied, and have not detected any evidence of any additional

polytypes. The most rapid and inexpensive method for spatial polytype mapping, especially when studying "mixed polytype" mesa samples, is thermal oxidation color mapping. The difference in dry oxidation rate between the respective silicon-faces of (0001) 4H-SiC and (111) 3C-SiC produces a sharp difference in oxide color following dry oxidation of a sample at 1150 °C for 5 to 7 hours.[11] Fig. 4a shows an optical micrograph of a "mixed polytype" mesa following thermal oxidation, whose formation is consistent with the simplistic illustrations depicted later in Fig. 10(f-j). The small light (nearly white) region corresponding to thinner oxide grown on 4H-SiC is the peak of an axial screw dislocation growth hillock, whose peak is poking through surrounding dark thicker oxide grown on 3C-SiC regions on the mesa.

2.2.2. Extended Defect Structure

In addition to polytype mapping, thermal oxidation also reveals where some kinds of extended crystal defects, such as SF's, intersect the silicon-face (111) 3C-SiC film surface.[11] The straight dark-line features in Fig. 4a are a result of enhanced oxidation where planar <111> stacking faults (inclined to the growth surface) intersect the top mesa surface. The other more disordered defects shown in Fig. 4a are DPB defects. The tendency for spoke-like patterns of DBP defects to form in 3C-SiC films surrounding axial screw dislocations (somewhat evident in Fig. 4a) is described in detail elsewhere.[17] In sharp contrast to the numerous defects apparent in Fig. 4a, Fig. 4b shows a typical 3C-SiC heterofilm nucleated on top of a step-free 4H-SiC mesa following thermal oxidation. The Fig. 4b film is completely free of SF and DPB extended crystal defects that are clearly revealed by the thermal oxidation of the mesa in Fig. 4a.

Although it is more destructive, defect-preferential etching is more capable of revealing crystal defects that intersect a film surface at a point (such as an axial screw dislocation or threading-edge dislocation) than thermal oxidation. Indeed, additional isolated dislocations beyond SF's and DBP's are revealed when 3C-SiC mesa heterofilms are subjected to defect-preferential molten KOH etching.[21] The differential interference contrast (DIC) optical micrograph shown in Fig. 5 is a typical comparison of the etch-pit morphology obtained from 3C-SiC heterofilms nucleated side-by-side on step-free (mesa (a)) and stepped (mesa (b)) 4H-SiC mesas. Etch pits are white features at the high morphology-contrast microscope settings used for Fig. 5. The SF-free 3C-SiC film nucleated on the step-free mesa (a) on the left exhibits five isolated triangular-shaped etch pits (denoted by white arrows). The defective 3C film on the stepped mesa (b) on the right exhibits far more abundant (10 to 100 fold) isolated triangular etch

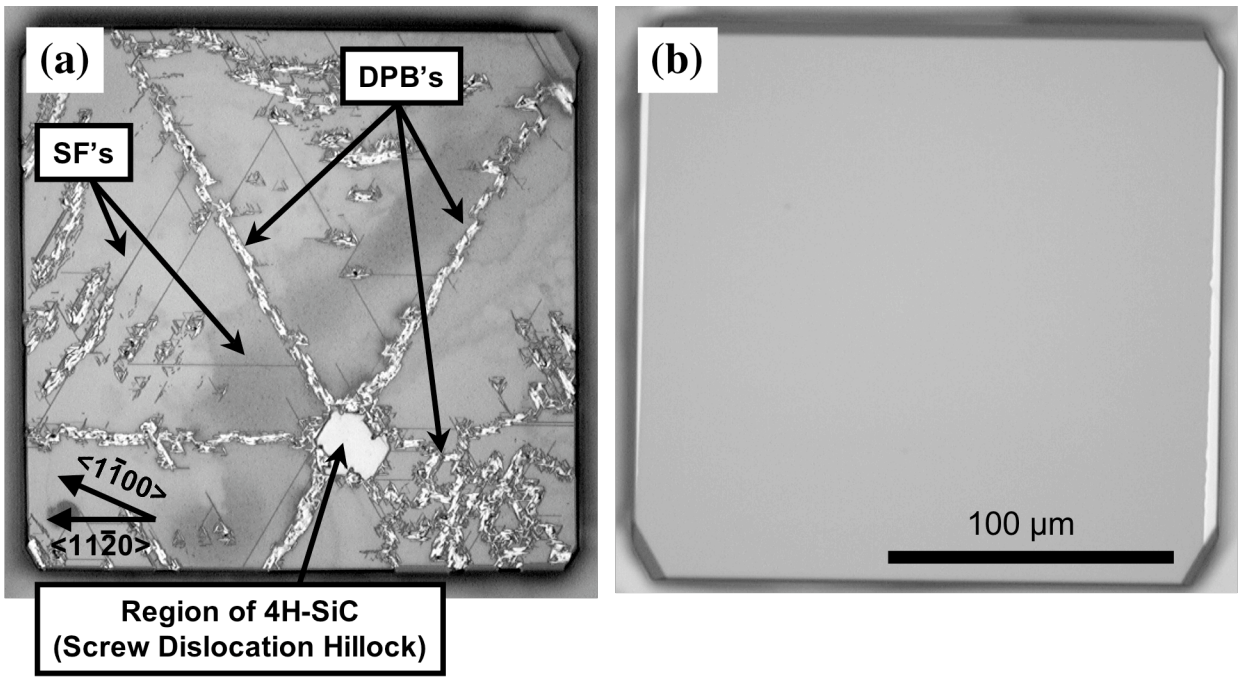

Fig. 4. Optical micrographs of oxidized 3C-SiC epitaxial films nucleated on (a) 4H-SiC mesa with steps from substrate axial screw dislocation (see Fig. 10 f-j) and (b) step-free 4H-SiC mesa (see Fig. 10 a-e)[17]. Difference in oxidation rate readily reveals the presence of 4H-SiC hillock peak and stacking fault (SF) and double-positioning boundary (DPB) defects on 3C-SiC film surface of film shown in (a), while 3C-SiC film shown in (b) is completely free of such defects.

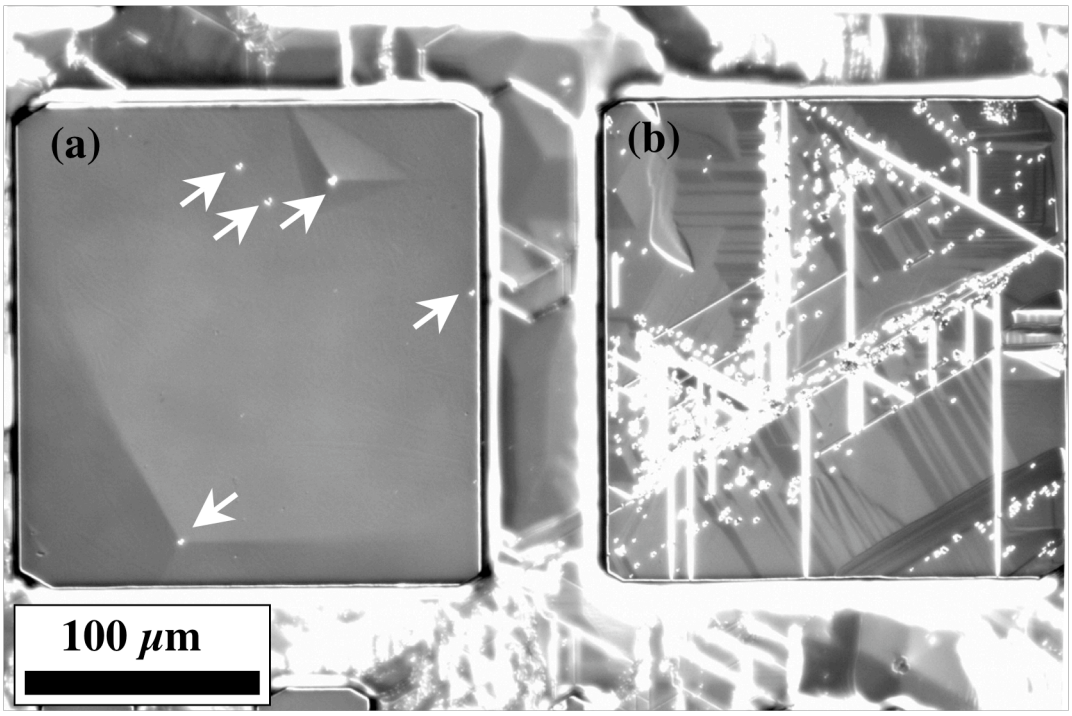

Fig. 5. Differential interference contrast (DIC) optical micrograph of side-by-side mesas showing dislocation-induced etch pits (white dots and lines) of two 3C-SiC heterofilms following defect-preferential etching in molten KOH. (a) 3C-SiC film nucleated on step-free 4H-SiC mesa, showing 5 isolated etch pits (highlighted by white arrows) and two tetrahedral growth hillocks. (b) 3C-SiC film nucleated on 4H-SiC mesa with steps showing abundant dislocation etch pits.

pits, in addition to line segment etch trenches that formed at SF defects. Comparable etch pit results were obtained for 3C-SiC heterofilms less than 4 μm thick,[21] as well as for 3C heteorfilms in excess of 10 μm in thickness.[21,27]

The Fig. 6 scanning electron micrographs (SEM's) detail three kinds of isolated pits observed following molten KOH etching. All isolated etch pits completely contained in 3C-SiC films were tetrahedral depressions into the surface with equilateral triangular pit sides aligned to $<1\bar{1}00>$ 4H-SiC substrate directions (Fig 6a). This shape is typical of dislocation etch pits commonly observed at threading edge dislocations in the (111) surface of cubic semiconductor crystals.[28] Isolated etch pits completely contained in 4H-SiC regions (of mixed poltype samples) were hexagonal with pointed bottom, as illustrated in Fig. 6b. Hexagonal etch pits

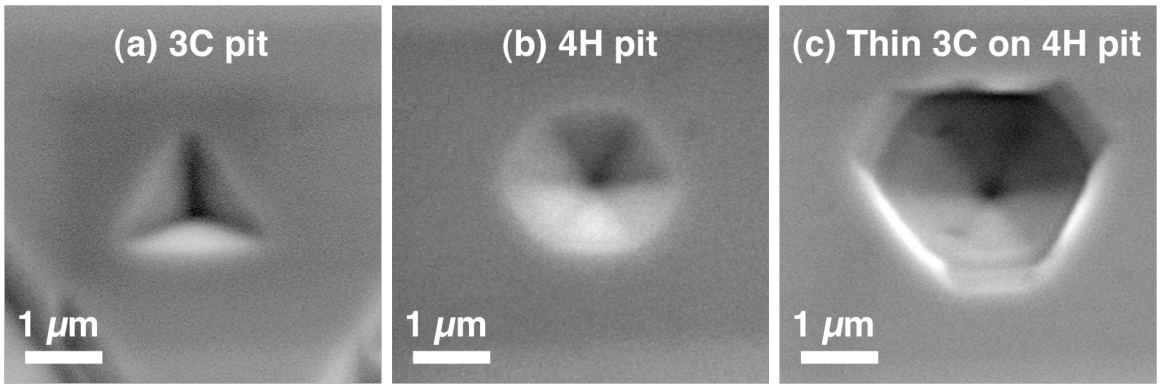

Fig. 6. SEM's of defect-preferential etch pits found in (a) 3C-SiC films, (b) 4H-SiC films, and (c) regions where defect-enhanced etching penetrated through entire thin 3C-SiC film and penetrating underlying 4H-SiC.[19]

always appeared at the peaks of hexagonal-faceted growth hillocks associated with axial screw dislocations. Additional hexagonal etch pits (with pointed bottoms) were also observed without associated growth hillocks, consistent with previously studied defect-preferential etching at threading edge dislocations in 4H-SiC.[29]

The pit morphology shown in Fig. 6c was observed when very thin SF-free 3C-SiC mesa films were KOH etched. The top portion of the Fig. 6c etch pit has partial triangular 3C character, while the deeper portion of the pit exhibits pointed-bottom hexagonal facet geometry. Such geometry, as well as the observed density on the order of 10^4 cm^{-2}, is consistent with propagation of threading-edge dislocations from the underlying 4H-SiC into the 3C heteroepilayer.[19] These results suggest that the majority of isolated etch pits present in SF-free 3C-SiC films grown on step-free 4H-SiC mesas (such as pits shown on mesa (a) in Fig. 5) originate from threading edge dislocations present in the underlying 4H-SiC.

The fact that much higher isolated triangular etch pit densities are usually observed for 3C-SiC films grown on stepped 4H mesas (Fig. 5 mesa (b)) indicates that the presence of steps on the initial 4H-SiC growth surface leads to an abundance of additional extended defects in the 3C-SiC film besides just SF's and DBP's. In contrast, high-quality 3C films grown on step-free

4H mesas lead to minimal additional dislocations (aside from pre-existing threading dislocations inherited from the underlying 4H-SiC) that propagate through the 3C film thickness to be revealed by defect-preferential etching.

One of the limitations of defect-preferential oxidation and KOH etching techniques is that these techniques cannot reveal dislocations confined to {111} planes parallel to and beneath the (111) 3C-SiC crystal top surface. To look for such defect structure buried beneath the 3C film surface, a few mesas were cross-sectioned and studied by HRXTEM. The typical results from one such mesa where 3C was grown on step-free 4H is shown in Fig. 7.[21] All SF-free 3C-SiC films studied by HRXTEM were structurally perfect with no defects and no stacking disorder detected throughout the 3C-SiC film thickness. The results confirm the growth model (Section 2.1) that there is strong thermodynamic preference for terrace nucleated bilayers to continue cubic stacking in these growth conditions, strongly refuting previous suggestions that hexagonal stacking might arise from random 3C variant terrace nucleation in standard SiC CVD growth

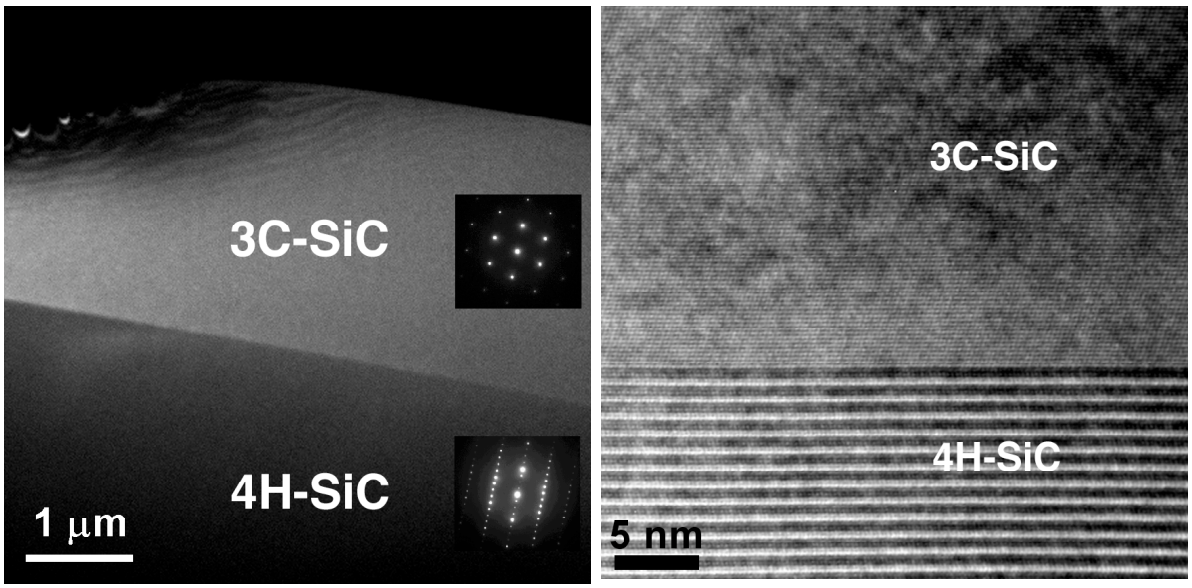

Fig. 8. HRXTEM of SF-free 3C-SiC heterofilm on 4H-SiC mesa (left) at low magnification and (right) high magnification.[21] No defects and no stacking disorder were observed in the 3C heterofilm, and the 3C/4H interface was atomically flat with no steps observed.

conditions below 1700 °C.[4,6] The 3C/4H interface was atomically abrupt and perfectly flat with no evidence of steps.

2.2.3. Surface Step Structure and Growth Rate

The fact that terrace nucleation is required to grow 3C-SiC films is fundamentally different from conventional epitaxial growth of 4H- and 6H-SiC films that require purely kinetic stepflow growth extension of existing steps (provided by surface miscut angle or axial screw dislocation spirals) without terrace nucleation. This naturally results in a fundamentally different growth surface, as well as quite different growth rates in some circumstances, for 3C-SiC mesa films.

Fig. 8a and 8b compare the AFM-observed growth surfaces from two nearby mesas of a mixed poltype sample that was grown as described by Neudeck et al.[30] as "Growth Run 2B". Fig. 8a shows the peak of an axial screw dislocation growth hillock on a 4H-SiC mesa where 3C-SiC failed to terrace nucleate (presumably due to high step density), while Fig. 8b shows the topmost terraces of a nearby mesa on the same sample where 3C-SiC nucleated on a step-free 4H-SiC mesa surface. Step heights of 0.5 nm (2-bilayers) and 1.0 nm (4-bilayers) are observed on 4H-SiC surfaces (such as surrounding spiral of Fig. 8a) in agreement with previous observations and models for hexagonal SiC on-axis growth.[8] SF-free 3C-SiC surfaces, such as those shown in Figs. 8b-d, exhibit single-bilayer height (0.25 nm) steps. Often, the topmost bilayers of 3C-SiC films are flat terraces with concentric step structure, such as shown in Fig. 8b. The clearly lower step density from the side-byside growth of the Fig. 8b 3C mesa compared to the Fig. 8a 4H mesa results from the fact that terrace nucleation is a probabilistic and non-instantaneous process. In order for terrace nucleation of a new bilayer island of 3C-SiC to occur,

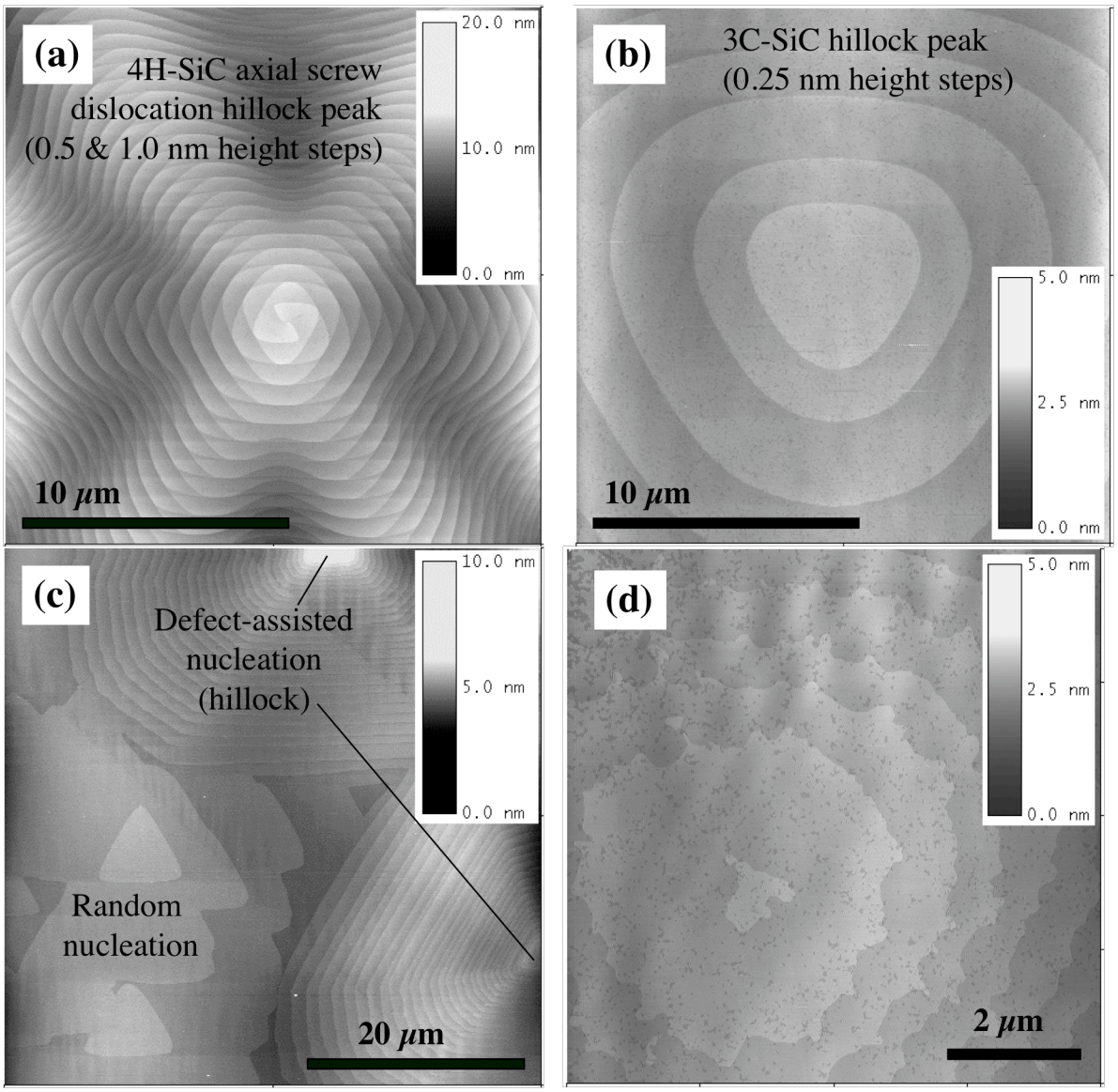

Fig. 8. Atomic force microscope (AFM) images of growth steps on SiC mesa surfaces. (a) 4H-SiC spiral growth emanating from axial screw dislocation. (b) Defect-assisted terrace nucleation growth of 3C-SiC, from nearby mesa on same sample as (a).[30] (c) Both defect-assisted and random nucleation on very thin (1 minute growth time) 3C-SiC film grown on step-free 4H-SiC mesa. (d) Terrace nucleation growth on same mesa as (b) following further growth under higher supersaturation (doubled silane and propane) growth conditions.[30]

a flat terrace surface (such as the topmost terrace in Fig. 8b) must enlarge to a sufficient degree that growth adatoms prefer to nucleate a new bilayer island instead of diffusing and incorporating into the existing step at the outer edge of the terrace. The higher step density of the

4H-SiC hexagonal hillock in Fig. 8a reflects the fact that spiral growth does not require terrace nucleation for new bilayers to be added to the crystal epilayer.

In the absence of spiral growth, a variety of other factors are known to impact terrace nucleation probability, and hence affect the growth rate and morphology of 3C-SiC films.[3,4,6,9] Defect-assisted terrace nucleation is known to occur when a crystal (terrace) surface contains a perturbation, such as a dislocation defect or surface contaminant, that locally lowers the free-energy at the interface and increases the probability for terrace nucleation of a new bilayer island to occur. The concentric steps evident in Fig. 8b are typical of what is observed at the top of 3C-SiC tetrahedral-shaped growth hillocks, consistent with a defect-assisted terrace nucleation process. KOH etching studies (discussed above) reveal that triangular etch pits form at the peaks of many such hillocks, consistent with the presence of a threading edge dislocation. For example, two such tetrahedral growth hillocks, both with KOH-etched pits at the peak, are evident in the DIC optical micrograph of the 3C-SiC mesa film shown in Fig. 5a. As shown in Fig. 8c, such hillocks are evident even at the very initial stages of 3C-SiC film growth. The Fig. 8c AFM shows the surface morphology of an extremely thin 3C-SiC film formed by only 1 minute of growth on top of a step-free 4H-SiC mesa surface (see Trunek et al.[31] "Sample C" for process details). The right side of the Fig. 8c AFM scan shows the sides of two tetrahedral growth hillocks that are beginning to form due to accelerated growth, producing clearly higher step density, compared to more random terrace nucleation growth evidenced in the lower left region of the AFM image.

Other defects, such as stacking faults, have also been documented to enhance the growth rate of 3C-SiC heterofilms, resulting in very large (sometimes > 100% max/min ratio) variations in 3C film thickness (i.e., effective growth rate) between adjacent mesas on the same sample.[31]

Growth process variables, such as temperature, pressure, and precursor flows, also critically affect local supersaturation and probability of terrace nucleation, and therefore the 3C-SiC film growth rate. Growth at higher supersaturation enables faster 3C-SiC film growth rates, higher step densities, and more uniform growth rates between mesas with and without extended crystal defects.[31] However, the structure of the step edges can become rougher than what is observed for lower supersaturation growth conditions.[30] As an example, Fig. 8d shows the AFM-measured film morphology of the same 3C mesa illustrated in Fig. 8b following additional growth under "higher supersaturation" conditions with doubled flows of silane and propane (see Neudeck et al.[30] "Growth Run 2C"). Additional interesting 3C-SiC growth surface observations are presented by Neudeck et al.[30], including nucleation of new bilayers at mesa edges/facets and observation of a 3C-SiC growth spiral.

2.2.4. In-Plane Lattice Mismatch: Strain and Relief

When growing films of one crystal on top of a different crystal, it is a well-known phenomenon that strain and relief effects arising from mismatch of in-plane lattice parameter have a large impact on heterofilm quality and properties.[24,32] A few previously published works have imprecisely stated that SiC lattice constants are the same for various polytypes. We have observed that lattice mismatch phenomenon applies to 3C on 4H SiC mesa heteropolytype crystals, even though the degree of mismatch is considerably smaller than most other heteroepitaxial crystal systems. More importantly, we have observed that remarkably benign lattice mismatch strain relief occurs for 3C- heterofilms grown on step-free 4H-SiC mesas, quite uniquely different from all previous strain relief observed to date in conventional heteroepitaxial crystals with atomically stepped heterointerfaces.

Extensive high-precision measurements of lattice parameters and relative in-plane lattice parameter mismatch have been conducted on 3C mesa heterofilms less than 4 μm thick by our co-authors at SUNY. Detailed quantitative procedures and results of the high-resolution x-ray diffraction (HRXRD) measurements are given elsewhere.[25,26,33] In summary, the SF-free 3C-SiC mesa heterofilms were found to be partially relaxed. The in-plane lattice constants of 3C-SiC mesa heterofilms were 0.01-0.08% greater than the in-plane lattice parameters of the underlying 4H-SiC mesas, yet still exhibiting some (~ 0.1%) in-plane compression from unstrained 3C unit cell dimensions. Given the HRXRD range of measured in-plane mismatch, simplistic calculations suggest that interfacial misfit dislocations might be expected every ~ 0.3 - 3 μm of in-plane distance along the 3C/4H interface. No rotational mis-orientation between the 3C film and 4H substrate was detected.

An initial high-resolution transmission electron microscopy (HRXTEM) study of 3C/4H interfacial misfit dislocation structure was conducted by our co-authors at Carnegie Mellon University (CMU) on a 15-μm thick 3C-SiC heterofilm grown on a step-free 4H-SiC mesa.[27] This thickness is well above the theoretically expected critical thickness of film relaxation expected for 3C/4H system. The Fig. 9 TEM shows that a well-ordered array of misfit dislocations is present near the 3C/4H SiC interface, with separation distance (i.e, density) within the range forecast by previous HRXRD studies (of other samples) and confirming that some film relaxation did indeed occur. Most remarkably however, molten KOH etching and HRXTEM analysis of this mesa show that aside from misfit dislocations buried at the 3C/4H interface, the 3C-SiC film is entirely free of any dislocations. Therefore, the step-free surface heteroepitaxy growth process enables remarkably benign relaxation of 3C/4H lattice mismatch resulting in greatly improved 3C-SiC heterofilm quality.

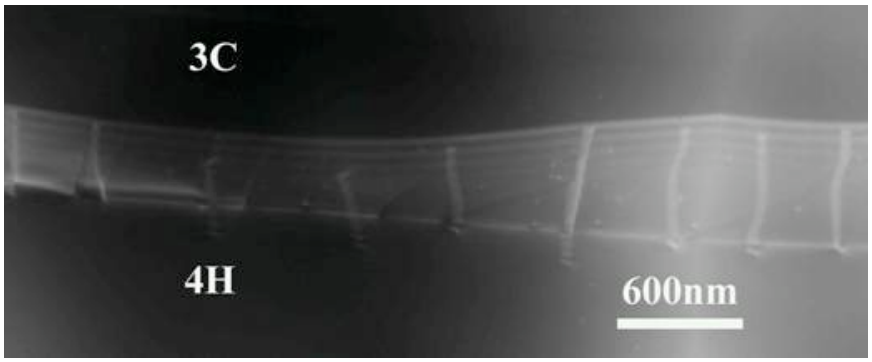

Fig. 9. TEM cross-sectional bright field image of the step-free 3C/4H interface with sample slightly tilted to reveal interfacial misfit dislocations.[27] Almost vertical line contrast corresponds to misfit dislocations at or near the 3C/4H interface plane. No dislocations were observed to propagate vertically into the 3C-SiC film.

The above result stands in sharp contrast to (and is quite inconsistent with) previously observed crystal heterofilm relaxation processes, which are known to produce abundant dislocations that are observed to propagate through thicknesses of cubic crystal-structure heteroepilayers.[32] Instead, our CMU co-authors proposed a new lattice mismatch relaxation mechanism wherein dislocation half loops nucleating at mesa edges and then gliding on planes parallel to the interface.[27] Relaxation by this previously unobserved mode does not leave threading dislocations propagating through the thickness of the 3C film. Thus, 3C-SiC mesa heterofilms have been used to start realizing the first prototype 3C-SiC diodes free of dislocations, producing record low-leakage and high breakdown electric field rectification properties.[34,35]

Interestingly, we have found that similar benefits are also realized when growing III-N heteroepitaxial films on step-free 4H-SiC mesas.[36,37] In contrast, 3C-SiC and 2H-AlN/GaN heterofilms grown on 4H-SiC mesas with steps exhibit highly disordered interface misfit dislocation structure coupled with 100X greater density of dislocations threading through the thickness of the heteroepilayers. These results indicate that the presence of steps at the

heteroepitaxial interface (i.e., on the initial heteroepitaxial nucleation surface) play a highly important role in the defect structure, quality, and relaxation mechanisms of single-crystal heteroepitaxial films. Investigations are continuing to more fully understand the full mechanisms by which atomic scale 4H-SiC steps generate abundant threading dislocations in 3C-SiC and 2H-AlN/GaN heterofilms.

3. Conclusions

This paper has highlighted important aspects of growth and characterization of high quality heteroepitaxial 3C-SiC films grown on step-free 4H-SiC mesas. Controlled nucleation on the step-free 4H-SiC mesa surface enables dramatic improvement in the structural quality of 3C-SiC heterofilms compared to growth on 4H-SiC mesas with steps, as verified by X-ray, TEM, AFM, thermal oxidation, and defect-preferential etching results summarized in this paper. Partial relaxation of 3C/4H in-plane lattice mismatch occurs via a unique (i.e., never before observed) mechanism that (in contrast to conventional relaxation mechanisms) completely avoids generation of dislocations through the 3C-SiC heterofilm. The superior film quality enabled by step-free surface heteroepitaxy opens opportunities to realize performance benefits from wide bandgap heterojunction devices previously limited by poor heterofilm quality. Potential applications include new heterojunction bipolar transistor structures and short-wavelength semiconductor lasers manufactured in low-defect III-N films on high thermally conducting SiC substrates.

4. Experimental

The simplified schematic cross-sections shown in Fig. 10(a-e) depict the basic growth process (for a single mesa) used to obtain the greatly improved 3C-SiC heterofilms.[17-20] Further experimental details of this process have been previously described in cited references. Starting from a commercially available on-axis silicon-face 4H-SiC or 6H-SiC wafer, arrays of mesas ranging in area up to 0.4 mm x 0.4 mm in dimension are defined across the wafer surface by etching trenches (depths ranging from as little as 5μm on some samples to as high as 25 μm on other samples) using standard photolithography and dry etching techniques (carried out at either NASA or the SiC wafer vendor).[38,39] After the etch pattern mask is stripped by wet chemical cleaning, this forms the schematic mesa cross-section shown in Fig 10a. It is important to note that a significant density of bilayer steps (depicted on the mesa top of Fig. 10a) will always be present on the surface of as-received commercial SiC wafers due to slight unintentional miscut and polish error, which is only specified as "on-axis" to within a few tenths of a degree of the (0001) basal plane.[38]

The wafer is then placed into a horizontal-flow cold-wall SiC epitaxial growth system[40] and subjected to a high temperature in-situ pre-growth etch to remove defects and contamination from the SiC growth surface. As first demonstrated by Powell et al.,[9] this pre-growth etch is critical to suppressing premature terrace nucleation, thereby enabling homoepitaxial growth of 4H-SiC and 6H-SiC despite extremely large terrace sizes that can evolve during "on-axis" homoepitaxial growth. HCl/H_2 mixtures (~1300 °C) and pure H_2 (1600-1650 °C) have been successfully employed towards this end in our experiments to date.[31]

Using growth conditions that completely suppress 2D terrace nucleation of 3C-SiC on large (hundreds of μm) basal plane terraces while carrying out stepflow homoepitaxy, device-

sized 4H/6H-SiC mesa regions with top surfaces completely free of atomic-scale steps can be grown.[18,41] As described more thoroughly in previous publications,[31,41] baseline growth conditions for this step have included 1600-1700 °C growth temperature, 2.7 – 5.4 cm^3/min SiH_4 and 0.3 – 9.0 cm^3/min C_3H_8 flowing in 4.4 l/min H_2 carrier gas at a pressure of 100 - 200 mbar.

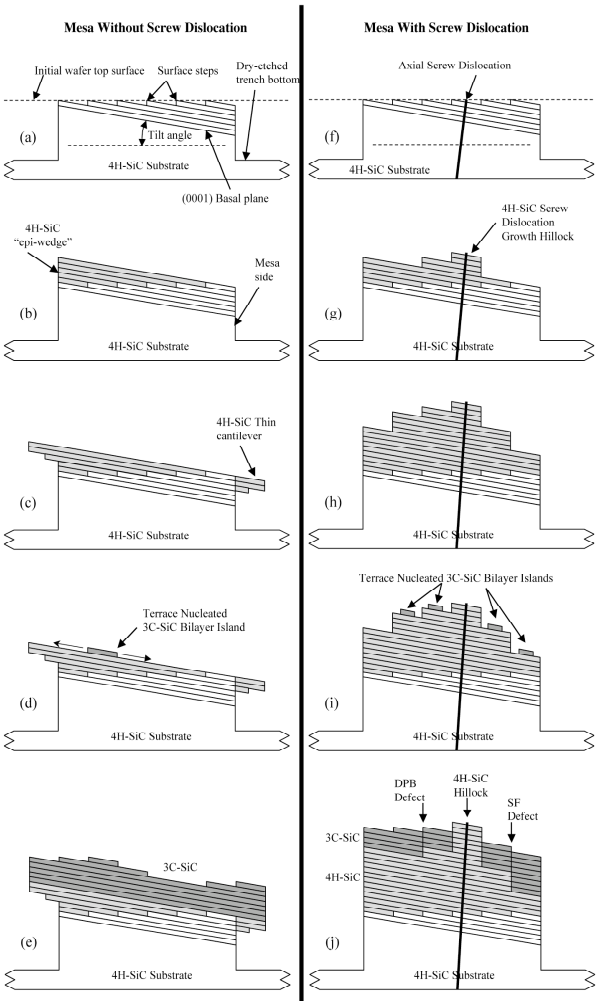

Fig. 10. Simplified cross-sectional depictions (showing bilayer planes) of on-axis mesa growth processes for left mesa without and right mesa with axial screw dislocation from the 4H-SiC substrate: (a & f) 4H-SiC mesa prior to growth. Pure stepflow growth with terrace nucleation supressed produces (b) step-free 4H-SiC mesa and (c) extension of thin 4H-SiC cantilevers on left mesa, while right mesa with screw dislocation evolves (g & h) hexagonal growth hillock. 3C-SiC heterofilm growth is initiated (d & i) via intentional terrace nucleation of bilayer islands that laterally expand via stepflow. Terrace nucleation is continued (e & j) to produce thicker 3C-SiC film.

The pure stepflow homoepitaxy with 2D terrace nucleation completely suppressed grows all initial surface steps over to the edge of the mesa. As shown in Fig. 10b, this leaves behind a step-free perfectly on-axis (0001) basal plane as the top surface of a 4H-SiC homoepilayer with a wedge-like thickness profile.

It is important to note that additional 4H-SiC bilayers cannot be added to an existing topmost (0001) terrace without axial screw dislocations (SD's) that provide a 4H polytype template and new growth steps. Instead, as illustrated in Fig. 10c, continued epitaxial growth of a screw-dislocation-free 4H-SiC mesa leads to the formation of thin lateral cantilevers that extend the step-free surface area from the top edges of some mesa sidewalls.[42,43] As depicted in Fig. 10(f-h) for mesas where SD's are present to provide a continuous spiral of new growth steps with polytype template, vertical growth of 4H-SiC continues without formation of cantilevers and the mesa never becomes free of surface steps.[17,41,42] Therefore, the random presence or absence of substrate axial screw dislocations within any given mesa enables 4H-SiC mesas with and without steps to be epitaxially produced side by side on any given wafer. Furthermore, comparing Fig. 10c cross-section to Fig. 10h cross-section, the presence or absence of cantilevers enables relatively easy optical microscope distinction between stepped and unstepped 4H-SiC mesas following homoepitaxial growth of sufficient duration.[42]

Once homoepitaxial growth has achieved step-free mesas (such as depicted in either Fig. 10b or Fig. 10c), heteroepitaxial nucleation of 3C-SiC can be initiated on top of the step-free 4H/6H-SiC surface in a controlled manner as schematically depicted in Fig. 10d.[17-20] We have named this process "step-free surface heteroepitaxy", as this reflects the nature of the 4H-SiC growth surface prior to 3C-SiC growth initiation. Most often, intentional terrace nucleation of 3C-SiC on the step-free 4H-SiC surface has been induced by gradually ramping the temperature

downward 50 to 200 °C without any other changes (or stopping of growth) from the conditions used to grow the step-free 4H mesa surfaces. The decreased growth temperature decreases surface adatom mobility, thereby increasing the probability of 2D terrace nucleation that initiates 3C-SiC growth. Consistent with well-known CVD crystal growth models, the terrace nucleation process initially forms a small Si-C bilayer island "nucleus" above a critical size that subsequently enlarges via stepflow expansion (Fig. 10d).[44] Terrace nucleation is then continued (Fig. 10e) to produce a thicker 3C-SiC film.

Acknowledgements

The work at NASA Glenn Research Center was carried out under the Ultra Efficient Engine Technology, Advanced Electrical Components, Revolutionary Aeropropulsion Concepts, and Director's Discretionary Funds projects. The authors wish to gratefully acknowledge the valuable assistance of Michelle Mrdenovich, Beth Osborn, Emye Benavage, Drago Androjna, Glenn Beheim, Gary Hunter, Lawrence Matus, David Larkin, Kimala Laster, Charles Blaha, Mike Artale, Jose Gonzalez, and Pete Lampard at NASA Glenn Research Center.

References

[1] A. R. Powell and L. B. Rowland, *Proc. IEEE* **2002,** *90*, 942.

[2] J. J. Sumakeris, J. R. Jenny, and A. R. Powell, *MRS Bulletin* **2005,** *30*, 280.

[3] J. A. Powell, P. Pirouz, and W. J. Choyke, in *Semiconductor Interfaces, Microstructures, and Devices: Properties and Applications* (Ed: Z. C. Feng), Institute of Physics Publishing, Bristol, United Kingdom **1993**, p. 257.

[4] H. Matsunami, *Jpn. J. Appl. Phys.* **2004,** *43*, 6835.

[5] M. H. Hong, A. V. Samant, and P. Pirouz, *Phil. Mag.* **2000,** *80*, 919.

[6] T. Kimoto, A. Itoh, and H. Matsunami, *Phys. Status Solidi B* **1997,** *202*, 247.

[7] H. Matsunami, K. Shibahara, N. Kuroda et al., in *Amorphous and Crystalline Silicon Carbide* (Eds: G. L. Harris and C. Y.-W. Yang), *Springer Proceedings in Physics, Vol. 34,* Springer-Verlag, Heidelberg, Germany **1989**, p. 34.

[8] J. A. Powell and D. J. Larkin, *Phys. Status Solidi B* **1997,** *202*, 529.

[9] J. A. Powell, J. B. Petit, J. H. Edgar et al., *Appl. Phys. Lett.* **1991,** *59*, 333.

[10] F. R. Chien, S. R. Nutt, W. S. Yoo et al., *J. Materials Research* **1994,** *9*, 940.

[11] J. A. Powell, J. B. Petit, J. H. Edgar et al., *Appl. Phys. Lett.* **1991,** *59*, 183.

[12] H. Nagasawa, K. Yagi, T. Kawahara et al., in *Silicon Carbide: Recent Major Advances* (Eds: W. J. Choyke, H. Matsunami, and G. Pensl), Springer-Verlag Berlin Heidelberg, Berlin **2003**, p. 207.

[13] V. Shields, K. Fekade, and M. Spencer, in *Silicon Carbide and Related Materials 1993* (Eds: M. G. Spencer, R. P. Devaty, M. Asif Khan, R. Kaplan, and M. Rahman), *IOP Conference Series*, *No. 137*, Institute of Physics, Bristol, United Kingdom **1994**, p. 21.

[14] M. Bhatnagar and B. J. Baliga, *IEEE Trans. Electron Dev.* **1993,** *40*, 645.

[15] G. Gao, J. Sterner, and H. Morkoc, *IEEE Trans. Electron Dev.* **1994,** *41*, 1092.

[16] K. K. Lee, Y. Ishida, T. Ohshima et al., *IEEE Electron Device Lett.* **2003,** *24*, 466.

[17] P. G. Neudeck and J. A. Powell, in *Recent Major Advances in SiC* (Eds: W. J. Choyke, H. Matsunami, and G. Pensl), Springer-Verlag, Heidelberg, Germany **2003**, p. 179.

[18] J. A. Powell, D. J. Larkin, P. G. Neudeck et al., United States Patent 5,915,194, **1999**.

[19] P. G. Neudeck, J. A. Powell, A. J. Trunek et al., in *Silicon Carbide and Related Materials 2003* (Eds: R. Madar, J. Camassel, and E. Blanquet), *Materials Science Forum, Vols. 457-460,* Trans Tech, Switzerland **2004**, p. 169.

[20] P. G. Neudeck, J. A. Powell, A. J. Trunek et al., in *Silicon Carbide and Related Materials 2001* (Eds: S. Yoshida, S. Nishino, H. Harima, and T. Kimoto), *Materials Science Forum, Vols. 389-393,* Trans Tech Publications, Switzerland **2002**, p. 311.

[21] P. G. Neudeck, J. A. Powell, D. J. Spry et al., in *Silicon Carbide and Related Materials - 2002* (Eds: P. Bergman and E. Janzen), *Materials Science Forum, Vols. 433-436,* Trans Tech Publications, Switzerland **2003**, p. 213.

[22] S. Nakamura, T. Kimoto, and H. Matsunami, *Jpn. J. Appl. Phys.* **2003,** *42*, L846.

[23] M. Dudley, W. M. Vetter, and P. G. Neudeck, *J. Cryst. Growth* **2002,** *240*, 22.

[24] M. J. Stowell, in *Epitaxial Growth, Part B* (Ed: J. W. Matthews), Academic Press, New York **1975**, p. 437.

[25] X. Huang, M. Dudley, P. G. Neudeck et al., in *Silicon Carbide 2002--Materials, Processing and Devices* (Eds: S. E. Saddow, D. J. Larkin, N. S. Saks, A. Schoener, and M. Skowronski), *Mater. Res. Soc. Symp. Proc., Vol. 742,* Materials Research Society, Warrendale, PA **2003**, p. K3.8.1.

[26] M. Dudley, X. Huang, and W. M. Vetter, in *Silicon Carbide: Recent Major Advances* (Eds: W. J. Choyke, H. Matsunami, and G. Pensl), Springer-Verlag, Berlin **2003**, p. 629.
[27] H. Du, M. Skowronski, P. G. Neudeck et al., to appear in *Silicon Carbide and Related Materials 2005* (Eds: R. P. Devaty, D. J. Larkin, and S. E. Saddow), *Materials Science Forum,* Trans Tech Publications, Switzerland **2006**.
[28] P. F. Kane and G. B. Larrabee, in *Characterization of Semiconductor Materials* McGraw-Hill, New York **1970**, p. 151.
[29] S. Ha, P. Mieszkowski, M. Skowronski et al., *J. Cryst. Growth* **2002,** *244*, 257.
[30] P. G. Neudeck, A. J. Trunek, and J. A. Powell, in *Silicon Carbide 2004--Materials, Processing and Devices* (Eds: M. Dudley, P. Gouma, T. Kimoto, P. G. Neudeck, and S. E. Saddow), *Mater. Res. Soc. Symp. Proc., Vol. 815,* Materials Research Society, Warrendale, PA **2004**, p. 59.
[31] A. J. Trunek, P. G. Neudeck, J. A. Powell et al., in *Silicon Carbide and Related Materials 2003* (Eds: R. Madar, J. Camassel, and E. Blanquet), *Materials Science Forum, Vols. 457-460,* Trans Tech, Switzerland, **2004**, p. 261.
[32] J. W. Matthews, in *Epitaxial Growth, Part B* (Ed: J. W. Matthews), Academic Press, New York **1975** p. 559.
[33] X. R. Huang, M. Dudley, W. Cho et al., in *Silicon Carbide and Related Materials 2003* (Eds: R. Madar, J. Camassel, and E. Blanquet), *Materials Science Forum, Vols. 457-460,* Trans Tech, Switzerland **2004**, p. 157.
[34] P. G. Neudeck, A. J. Trunek, and D. J. Spry, to appear in *Silicon Carbide and Related Materials 2005* (Eds: R. P. Devaty, D. J. Larkin, and S. E. Saddow), *Materials Science Forum,* Trans Tech Publications, Switzerland **2006**.
[35] D. J. Spry, A. J. Trunek, and P. G. Neudeck, in *Silicon Carbide and Related Materials 2003* (Eds: R. Madar, J. Camassel, and E. Blanquet), *Materials Science Forum, Vols. 457-460,* Trans Tech, Switzerland **2004**, p. 1061.
[36] N. D. Bassim, M. E. Twigg, C. R. Eddy, Jr. et al., *Appl. Phys. Lett.* **2005,** *86*, 021902.
[37] N. D. Bassim, M. E. Twigg, M. A. Mastro et al., to appear in *Silicon Carbide and Related Materials 2005* (Eds: R. P. Devaty, D. J. Larkin, and S. E. Saddow), *Materials Science Forum*, Trans Tech Publications, Switzerland **2006**.
[38] Cree, Inc., http://www.cree.com.
[39] G. M. Beheim and C. S. Salupo, in *Wide-Bandgap Electronic Devices* (Eds: R. J. Shul, F. Ren, M. Murakami, and W. Pletschen), *Mater. Res. Soc. Symp. Proc., Vol. 622,* Materials Research Society, Warrandale, PA **2000**, p. T8.9.
[40] Aixtron GmbH., http://www.aixtron.com.
[41] J. Powell, P. Neudeck, A. Trunek et al., *Appl. Phys. Lett.* **2000,** *77*, 1449.
[42] P. G. Neudeck, J. A. Powell, G. M. Beheim et al., *J. Appl. Phys.* **2002,** *92*, 2391.
[43] P. G. Neudeck and J. A. Powell, United States Patent 6,461,944, **2002**.
[44] T. Kimoto and H. Matsunami, *J. Appl. Phys.* **1994,** *75*, 850.